Nanoscale

Accepted Manuscript

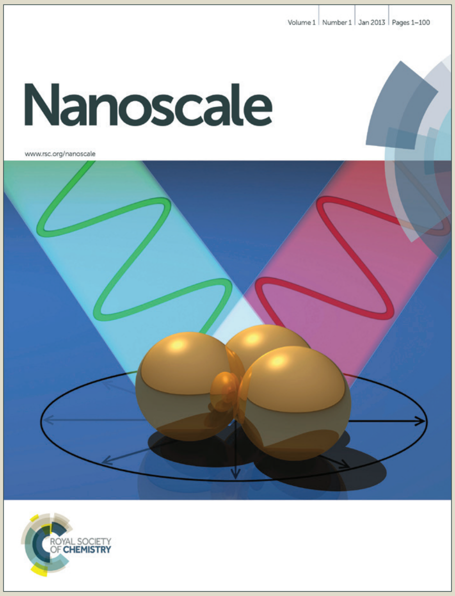

ROYAL SOCIETY OF CHEMISTRY

www.rsc.org/nanoscale

Nanoscale RSCPublishing

ARTICLE

Improved Heterogeneous Electron Transfer Kinetics of Fluorinated Graphene Derivatives

Cite this: DOI: 10.1039/x0xx00000x

Sidhureddy Boopathi,[a] Tharangattu N. Narayanan, [a]* and Shanmugam SenthilKumar[a]*

Received 00th January 2012,
Accepted 00th January 2012

DOI: 10.1039/x0xx00000x

www.rsc.org/

Though graphitic carbons are commercially available for various electrochemical processes, their performance is limited in terms of various electrochemical activities. Recent exposure on layered carbon materials, such as graphene, demonstrated an augmented performance of these systems in all electrochemical activities due to their unique electronic properties, enhanced surface area, structure and chemical stabilities. Moreover, flexibility in controlling electronic as well as electrochemical activities by heteroatom doping brings further leverage in their practical use. Here, we study the electron transfer kinetics of fluorinated graphene derivatives, known as fluorinated graphene oxide (FGO) and its reduced form, RFGO. An enhanced electron transfer kinetics (heterogeneous electron transfer (HET)) is observed from these fluorinated systems in comparison to their undoped systems such as graphene oxide (GO) and reduced GO. A detailed study has been conducted using standard redox probes and biomolecules revealing the enhanced electro-catalytic activities of FGO and RFGO, and electron transfer rates are simulated theoretically. This study reveals that fluorine is not only inducing defects in graphitic lattice leading to an enhanced HET process but also can modify the electronic structure of graphene surface.

Introduction

Carbon is established as an ideal electrode material for electronic as well electrochemical sensors and devices due to its easy availability, chemical inertness, wide anodic potential range, low residual current, fast response, ease in fabrication of different sizes and configurations, and reduced cost.[1] Different forms of carbon namely; glassy carbon, [2] highly oriented pyrrolitic graphite (HOPG),[3] carbon paste,[4] carbon nanotubes (CNTs),[5] and graphene [5] were emerged as electrode materials for various sensors and devices. Out of these various forms, graphene, atomically thin carbon sheet with sp^2 carbons distributed in a honeycomb fashion, is highly researched for its advanced sensing and electron transfer properties, in the recent past.[3,4]Along with its very high mobility (~ 200,000 $cm^2/V.s$), high surface area (2630 m^2/g), metal free basal and active edge planes enable graphene as ideal for the development of high efficient electron transfer systems such as sensors. [6–8] Various types of graphene based sensors were developed in the recent past, and role of edge and basal planes of graphene in determining the effective sensitivity is also subjected to study.[9] But in a recent report, it is established that apart from the effects of basal and edge planes of graphene in net electron transfer process, its atomic thickness and structure are insignificant in electron transfer process, and for instance, the electrochemical response will not vary much from single to few layers of graphene.[10]

Doping can modify the electronic structure of graphene, and it can also bring interesting physico-chemical properties to the graphitic system.[11–13] Various functional derivatives of graphene have been synthesized *via* doping, and fluorinated graphene (FG) is one among them.[14,15] Fluorination of graphene will introduce sp^3 carbon in sp^2 honeycomb matrix, and will alter the electronic structure of graphene. Moreover, highly electronegative fluorine can change the surface properties of graphene with a high thermal stability in to the structure.[16] Recently, some of these authors studied various multifunctional properties FG derivatives, and came up with a green synthesis route towards the development of bulk amount of FG.[17] In this study, we report a phenomenal enhancement in the electron transfer properties of graphene upon fluorine incorporation, and unraveling the fundamental mechanism underlying in this enhanced heterogeneous electron transfer (HET) process with the aid of detailed electrochemistry analysis and computational simulation. Detailed HET studies on fluorinated graphene oxide (FGO) (a functional derivative of FG, containing various oxygen functionalities) and Reduced fluorinated graphene oxide (RFGO) were conducted for the first time with a negatively charged redox molecule namely $[Fe(CN)_6]^{3-/4-}$.

Extensive studies on the HET processes on glassy carbon and HOPG surfaces were made by McCreery *et al*[1, 2] But unlike these systems, the electrochemistry of graphene needs to be understood on giving due considerations to several other factors such as conductivity (way of synthesis), percentage and nature of defects, presence of functionalities, orientation and presence of other elements.[18,19] Graphene oxide (GO), an oxygen rich functional derivative of graphene,[20] is considered as a base material for the bulk synthesis of graphene by various reduction methods. But, graphene produced in this method may contain residual functional groups and defects such as Stone-Wales type.[21] These may can alter the resultant HET process.[22,23] Extent of reduction and nature of reduction method carried out will affect the resultant end products, and hence a notable variation in HET rate constant of graphene is observed in different reports [24,25]. But HET studies on similarly synthesized fluorine doped graphene oxide systems were not carried out in literature and such a study will fundamentally probe the electron transfer mechanism.

Experimental Section

Synthesis of GO, RGO, FGO and RFGO: GO has been synthesized using “Improved Synthesis” method.[17] 9:1 mixture of concentrated H_2SO/H_3PO_4 (360:40 mL) was added to a mixture of graphite flakes (3.0 g, 1 wt equiv, SP-I Bay carbon) and $KMnO_4$ (18.0 g, 6 wt equiv). The reactants were then heated to 50°C and stirred for 12 h. The reaction was cooled to room temperature and poured onto ice with 30% H_2O_2 (3 mL). The material was then washed in succession with 200 mL of water, 200 mL of 30% HCl, and 200 mL of ethanol (2 times). The material remaining after this multiple-wash process was coagulated with 200 mL of ether, and the resulting suspension was filtered over a PTFE membrane with a 0.22 µm pore size. Fluorinated GO (FGO) has also been prepared using a similar method taking fluorinated graphite polymer (Alfa Aesar 42537) as the starting material and scooping the phase separated top part, as it is reported in the previous work. [1] Both GO and FGO are subjected to a controlled thermal reduction at 90°C under hydrazine hydrate atmosphere for 12 hours in vacuum oven to get graphene (RGO) and FG.

STEM measurements were carried out using JEOL 2100 Field Emission Gun Transmission Electron Microscope and micro Raman analysis was carried out using Renishaw Raman Microscope. Raman analysis was carried out on the powder samples with 633 nm laser excitation. Laser intensity was kept ~1% and the exposure time was 30 seconds. A 50x lens was used to focus the laser beam. Bruker FT-Infrared instrument used to conduct FT-IR measurements. Bruker FT Nuclear Magnetic Resonance (NMR) spectrometer (400 MHz) was used for ^{19}F NMR spectrum acquiring.

Fabrication of graphene electrodes: 2.5 mg of synthesized graphene material was dispersed in 500µl millipore water and 5µl of these dispersed aliquots drop casted on well-polished glassy carbon (GCE) surface for the modification. Then electrodes were allowed for 30min for drying. These modified electrodes were used for all the electrochemical experiments. The geometrical area of GCE(BASi Analytical Instruments) is $0.07 cm^2$.

Electrochemical Studies: CHI instrument Inc. (model no. 900B) was used for all potentiodynamic experiments. Heterogeneous electron transfer studies performed on different types of GO modified electrodes using cyclic voltammetry in aqueous electrolyte 1 M KCl containing 1 mM $K_3[Fe(CN)_6]$ solutions at the scan rate of 0.1V/s from the switching potential range between 0.2V to 0.6V. BAS-IM6 was used to get Nyquist plot of the Electrochemical impedance spectroscopy at formal potential in aqueous electrolyte 1 M KCl containing 1 mM $K_3[Fe(CN)_6]$ solutions, frequency range from 100kHz to 0.05Hz. Ag/AgCl reference electrode was used for entire electrochemical studies. A three electrode cell set up was used for cyclic voltammetry.

Computational simulations studies: Digielch electrochemical simulation software (Digielch 7 professional V7, Model No: 987-00076) was used for the simulation of electrochemical experimental results.

Results and Discussion

In the present investigation, 4-different systems namely - fluorinated graphene oxide (FGO), GO, Reduced fluorinated graphene oxide (RFGO) and graphene (reduced graphene oxide, RGO) – were subjected to HET studies. Detailed structure and synthesis procedure of each of these materials were discussed in our previous reports and briefly explained in the experimental section. In a nutshell, all these materials were synthesized *via* the same chemical route and reduction of oxide systems have been conducted in a similar fashion to ensure the same extent of reduction of oxygen functionalities. Similar to our earlier reports and many other reports, all these materials are layered 2-dimensional (2D) materials containing 1-2 atomic layer thickness, similar BET surface area (BET surface area of powder samples ~140-150 m^2/g) and lateral width. High angle annular dark field image of FGO collected using a scanning transmission electron microscope is shown in figure 1A. Atomic layering is evident from this image. This FGO contains ~ 23% of F by atomic percentage (64.61% Carbon and 11.45% Oxygen). Thermal treatment of FGO with hydrazine vapours results in to the reduction of its oxygen functionalities giving rise to a reduced form known as RFGO (details of reduction procedure are given in the experimental section and extent of reduction is discussed in the next section).

FT-IR spectra of all these samples were shown in figure 1B. All particulars of functional groups are reported in our previous reports. In particular, the characteristic difference between fluorinated and non-fluorinated samples is the presence of C-F bond in fluorinated samples at 1204 cm^{-1}. Moreover, the similar reduction of GO and FGO leads to the same extent of removal of oxygen functional groups, as it is clear from the FTIR spectra of reduced samples (RGO and RFGO). In the case of

RGO and RFGO also the major difference in the amount of functional groups is only in C-F. This indicates that except the presence of fluorine, the chemical structure of both RGO and RFGO are same. ^{19}F NMR spectrum of FGO is recorded after dispersing FGO powder in chloroform, and the details are shown in supporting information. The NMR spectrum shows two distinct peaks placed near ~ -180 ppm, indicates the presence of covalent C-F bonds. Further, ^{19}F NMR also shows the presence of tertiary alkyl fluorides and confirms the presence of large number of fluorine in the basal plane than at the edges.

For further probing the nature of defects present in these systems, a detailed micro-Raman analysis is performed and the results are appended in the Figure 1C. It is clear from the Raman analysis and from our earlier studies that the samples show clear signatures of graphitization in RFGO and RGO, relatively high sp^3 content in RFGO is due to the presence of large number of fluorine.

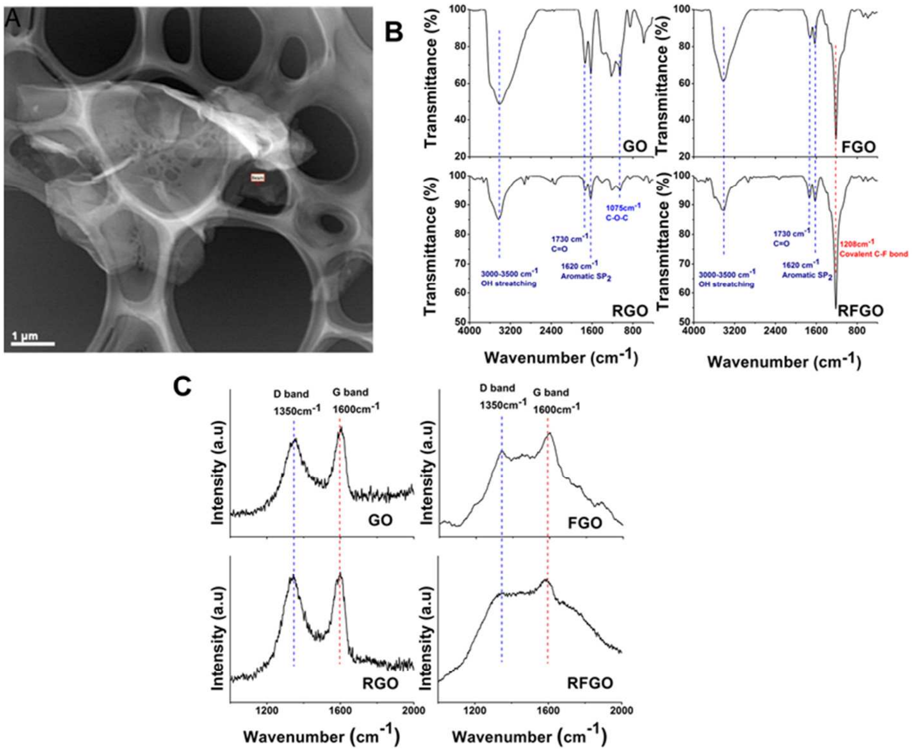

Figure 1 A. High Angle Annular Darkfield image of FGO, showing the atomically thin layered structure of FGO. 1B) FTIR spectra of different graphene oxide, 1C) Raman spectra of different graphene oxide

Electrochemistry of GO/RGO and FGO/RFGO were studied using cyclic voltammetry (details of the experiment are given in the experimental section) and electrochemical impedance spectroscopy. Figure 2(A-D) shows the comparison of cyclic voltammogram (CV) of graphene oxide based electrodes (electrode synthesis is explained in the experimental section) in mixture of 1mM $K_3[Fe(CN)_6]$ and 1M KCl solutions at a scan rate of 0.1V/s. A quasi-reversible, negatively charged redox molecule, named potassium ferricyanide, is used for HET studies. GO is showing negligible current for the HET of $[Fe(CN)_6]^{3-/4-}$ and its corresponding redox peak potential difference is around 0.2V (figure 2A). It indicates that GO is blocking the HET electron transfer due to electrostatic repulsion between negatively charged ferricyanide species[24] and it behaves like an insulating material due to the presence of large varieties of oxygen containing functional groups such as -C=O, -COOH, -CHO, -OH and etc. It has been established that oxygen functional groups present in GO may lead to the electrostatic repulsion resulting to a larger electron tunneling distance and more sluggish kinetics. [24]

A similar study has been conducted on FGO (figure 2B). Remarkably, FGO is showing a well-defined peak at 0.220 V corresponding to the HET of $[Fe(CN)_6]^{3-/4-}$ with redox peak potential difference 0.11 V. It is assumed that FGO, having lot of oxygen containing functional groups with covalent C-F bond: hence it is expected to retard the HET, will act like GO in HET process. Contradicting to this expectation, FGO behaves like a very good electrode materials than GO. This observation leads to the conclusion that fluorine is playing a seminal role in distinguishing these HET processes in these two materials, otherwise similar in terms of chemical (except the presence of fluorine in FGO) and physical structure.

Next we have compared the cyclic voltamograms (CV) of RGO and RFGO with GO and FGO. These reduced form of graphene oxides are showing higher peak current and low redox peak potential difference (figure 2C & 2D) than its corresponding unreduced form of graphene oxides in HET process. It indicates that functional groups are substantially got removed (as seen in FT-IR spectra) after the hydrazine reduction and they are playing a key role in hindering the electron transfer process and this correlates with others observations. [24] Though there are some contradictory arguments on the role of functional groups on the carbon process in the HET process, this enhanced electron transfer process in the case of reduced systems are may be due to the reduced negative charge and enhanced electronic conductivity. [26,20] However there is no study has been conducted so far to correlate the conductivity of modified electrode materials and their heterogeneous electron transfer.[27]

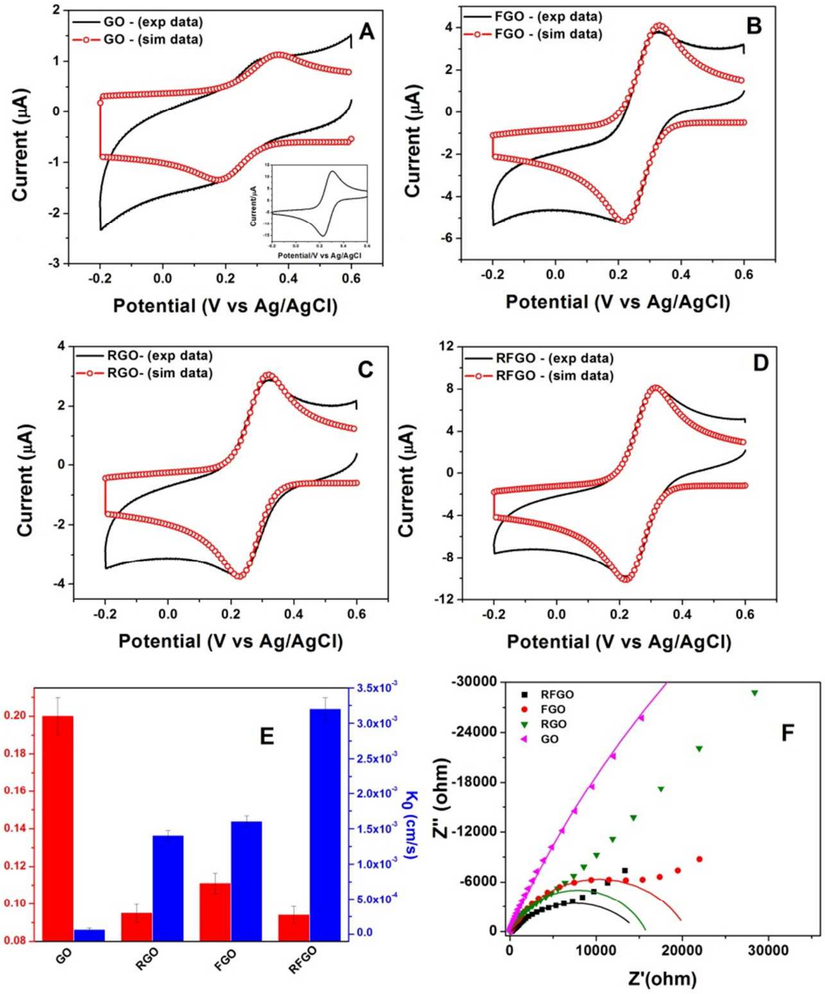

Figure 2. Cyclic voltammograms obtained using different graphene oxide material (A-GO, B-FGO, C- RGO, D- RFGO) modified on glassy carbon electrode at scan rate of 0.1V/s in aqueous electrolyte 1 M KCl containing 1 mM $K_3[Fe(CN)_6]$ solutions (black line-experimental data, Red colour circle –simulation data). (A) Inset: Bare GCE cyclic voltammogram obtained in the above mentioned conditions. (E) Plot of anodic and cathodic peak potential difference of $[Fe(CN)_6]^{4-/3-}$ and rate constant values of different GO surfaces. (F) Nyquist plot obtained using EIS measurements of different GO surfaces in aqueous electrolyte 1 M KCl containing 1 mM $K_3[Fe(CN)_6]$ solutions from 100kHz to 0.05Hz. Dotted curve is experimental data; solid line corresponds to fitted semi-circle curve.

Additionally HET process is simulated using a Digielch 7 professional V7 software. Here, experimental parameters were used to simulate the CV for the four samples (GO, FGO, RGO and RFGO) and fitted faradaic portion of the experimental data. The HET rate constants (K^o) were determined through digital simulation of cyclic voltammetric i-v curve (details of experimental parameters are given in the experimental section). Comparing the HET rate constants, it is observed that HET rates follow the following order: RFGO ($3.2x10^{-3}$) > FGO ($1.6x10^{-3}$) > RGO ($1.4x10^{-3}$) > GO ($6.2x10^{-5}$). For clear understanding, the averaged redox peak potential difference and obtained HET rate constant of $[Fe(CN)_6]^{4-/3-}$ at various forms of graphene oxide shown in figure 2E. It indicates that fluorine is playing an significant role in HET processes apart from oxygen functional groups effects in slowing down the electron transfer kinetics.

Further, we probed the surface chemistry of these GO materials with benefit of electrochemical impedance spectroscopy (EIS) to evaluate HET resistance between the electrode material and $[Fe(CN)_6]^{3-/4-}$. EIS performed at the formal potential of

$[Fe(CN)_6]^{3-/4-}$ to measure the charge transfer resistance of different samples (figure 2F). GO exhibits a higher charge transfer resistance of around 233 kΩ due to its high amount of oxygen functionalities with large number of sp^3 domains. But FGO showing less charge transfer resistance (~20.53 kΩ) than GO, even with the presence of oxygen containing functional groups (similar amount, FT-IR) on its surface. EIS data is in consistent with the cyclic voltammetry results. Fluorine doped systems show high amount of defects density so that these defects may responsible for enhanced HET process. This is in tune with a very recent report by Pumera et al where they showed the enhanced HET kinetics with the amount of fluorine in fluorinated graphite polymers.[28] In the case of RGO (15.8 kΩ) and RFGO (14.6 kΩ), the lower R_{ct} was observed than those corresponding unreduced forms of graphene oxides. This HET resistance reflects in low redox peak potential difference (ΔEp) of molecular probe $[Fe\ (CN)_6]^{3-/4-}$ cyclic voltammetry. The chemical reduction of GO/FGO will introduce additional defects on honeycomb lattice in the form of dangling bonds, stone-wales defects and formation of large number of small sp^2 domains.[29] These additional defects may responsible for enhanced electron transfer kinetics in reduced systems. In addition, the reduction of oxygen functionalities will also improve the electronic conductivity of the materials.

Hence, in the case of fluorine graphene derivatives, presence of large number of defect sites arising due to the presence of fluorine and other oxygen functionalities, (as can be seen in Raman data) is the responsible for the augmented HET process. Further, the presence of fluorine in the graphitic matrix is reduces the surface energy and hence make the surface more hydrophobic.[17] Hence, even oxygenated FGO has been reported for its amphiphobic properties by some of the authors. Hence the negatively charged redox molecule won't get repelled by the electrode though it contains negatively charged oxygen functionalities.[30] This is also one of the potential possibilities for the improved heterogeneous electron transfer properties of FGO. Recently, Pumera et al reported that HET kinetics of halogenated graphene oxides, where the electron transfer rate increases with the decrease in atomic number of the doped halogen (transfer rates track the following order, Cl-TRGO > Br-TRGO > I-TRGO) (where TRGO means thermally reduce graphene oxide)). [31] In the present work, the HET rates obtained for RFGO is $3.2x10^{-3}$ cm/s. This value is higher than that reported for Cl-TRGO ($2.52x10^{-3}$ cm/s). Hence, this also proves the role of atomic weight of doped element in graphene oxide materials for determining the resultant HET.

The electro oxidation of biologically important molecules such as ascorbic acid (AA), dopamine (DA), and uric acid (UA) using graphene electrodes are always depend on the alignment of graphene electrodes and the nature of functional groups present on graphene surfaces.[11] By studying these kinds of biomolecule's electrocatalytic behavior on FGO, one can understand the intrinsic properties of FGO surface. Figure 3 (A-C) shows the CVs of 1.0 mM AA, DA, and UA oxidation in PBS 7.4 at different graphene oxide materials modified glass carbon electrode. AA oxidation is chemically irreversible process and the electrode kinetics depend on oxidation potential (Ep_{ox}). It can be seen from figure-3A that the AA oxidation is fully hindering in the present experiment with GO surface and this can be due to the electrostatic repulsion between rich oxygenated functional group containing GO and negatively charged AA molecule. Unlike GO, RGO shows AA oxidations and anodic peak current start at 0.2 V indicating hydrazine reduction leads to the effective removal of oxygenated functional. Interestingly, in the case of FGO modified GC electrode shows significantly lower over potential with anodic peak current start at 0.0 V indicating fast electron transfer kinetics (0.2 V less anodic shifts in oxidation potential than RGO), even with the presence of more oxygen containing functional groups than that in RGO. In the case of RFGO, AA oxidation peak starts at the same potential of 0.0 V and only

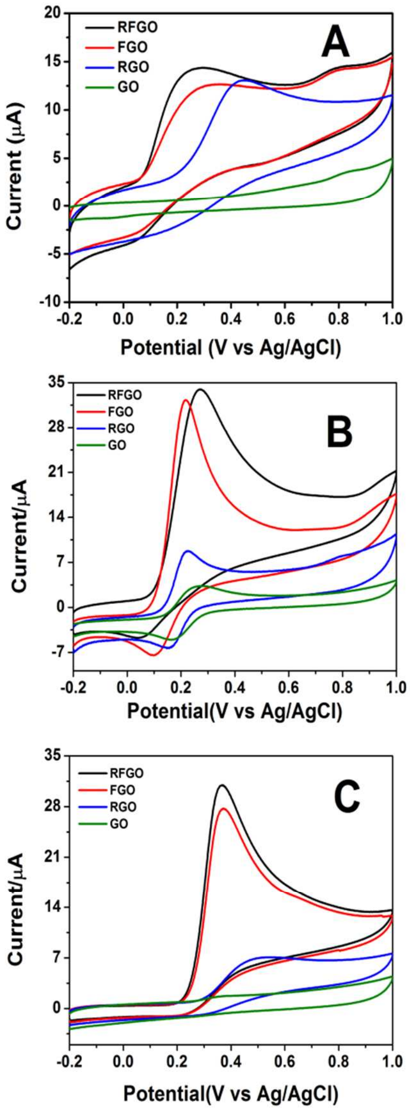

Figure 3. Cyclic voltammograms obtained in functionalized GO surface in PBS (pH 7.4) containing (A) 1 mM ascorbic acid (B) 1 mM dopamine (C) 1 mM uric acid solutions at scan rate of 0.1 V/s.

small peak current (2 μA) enhancement observed than FGO surface. It indicates no such great influence on oxygen functional present on FGO surface. As appeared in previous literature, AA oxidation is a surface sensitive electrochemical reaction[2], i.e., sensitive to surface chemistry and microstructure as well as density of electronic states near the formal potential.[1,32] Unlike AA, DA oxidation peak is noticeable at even GO surface (figure-3B). This is because of electrostatic attraction between negatively charged GO surface and positively charged DA molecule in PBS 7.4 condition. The RGO surface has higher DA oxidation starts at 0.1 V and peak current is 10 μA. In the case of FGO, superior catalytic activity was observed for DA oxidation, in term of less anodic over potential (0.05 V) with 3.3 times (33μA) higher current than GO surface. Like AA oxidation, DA oxidation at RFGO surface also not much affected in terms of oxidation potential and peak current compared to FGO. But it is established that DA is less insensitive to the surface oxygen functional groups on graphene surface, and hence this study reveals that fluorine doping on graphene oxide may have a prominent role in altering the density of electronic states near Fermi level.

Finally, we studied UA oxidation on different GO surface and shown in figure 3C. UA is also negatively charged molecules in PBS (pH-7.4) condition and it also repels as like AA molecule on GO surface and no characteristic oxidation behaviour was observed on GO. However, in the case of FGO surface UA oxidation peak starts at 0.208 V (0.090 V less anodic shifts in oxidation potential than RGO)) with 4.5 times higher current than RGO was observed. This also further confirms the surface of FGO has high catalytic nature than GO, and RGO. The enhancement of fast electron transfer kinetics of AA, DA and UA on RFGO and FGO is probably due to the abundant microstructure, defects and density of electronic states near the formal potential. Some theoretical work is needed for understating the electronic states of fluorine doped graphene oxide and these studies are in progress. Moreover, the electrochemical studies on fluorinated graphene derivatives indicate that fluorine not only changing the physico-chemical properties of graphene surface, it may also alter its electronic and magnetic properties, and it is in accordance with our earlier studies on similar fluorinated systems.[33]

Conclusions

A detailed electrochemical study has been conducted on various functional derivatives of doped and undoped graphene oxide surface to prove the role of defects in determining the net electron transfer kinetics. It is observed that the presence of fluorine in graphene oxide surface induces more defects on graphitic surface leading to an enhanced HET kinetics than the undoped counter parts. Moreover, this study also reveals that fluorine can also alter the electronic states of graphene surface. The observed less anodic over potential and higher peaks currents for electrooxidation of biologically important molecules of AA, DA and UA with FGO/RFGO surfaces indicate the efficient electro catalytic nature of fluorinated materials than GO and RGO electrodes. This study open the possibilities for making fluorinated graphene derivatives based point of care systems, and also open a new avenue for the fundamental studies on electron transfer properties of various electrodes on the basis of nature dopants.

Acknowledgements

Among the authors, SB thanks CSIR for the SRF fellowship. TNN acknowledges the financial support from CSIR-CECRI in the form institution start-up fund (OLP 0087) and also acknowledges DST for financial support in the form of DST-FAST Track scheme (SB/FTP/PS-084/2013: GAP26/13). SS acknowledges CSIR-Multifun (CSC0101). TNN acknowledges Prof. P. M. Ajayan, Rice University for his support.

Notes and references

[a] CSIR-Central Electrochemical Research Institute (CSIR-CECRI) Karaikudi-630006, India.
*tn_narayanan@yahoo.com (T. N. N.) [Corresponding & Communicating author]
* ssenthilmugam@gmail.com (S.S.K)

1 McCreery, R. L. *Chem. Rev.* 2008, **108**, 2646.
2 Chen, P.; McCreery, R. L. *Anal. Chem.* 1996, **68**, 3958.
3 Pumera, M. *Chem. Soc. Rev.* 2010**, 39**, 4146.
4 Ratinac, K. R.; Yang, W.; Gooding, J. J.; Thordarson, P.; Braet, F. *Electroanalysis* 2011, **23**, 803.
5 Silva, T. A.; Zanin, H.; Saito, E.; Medeiros, R. A.; Vicentini, F. C.; Corat, E. J.; Fatibello-Filho, O. *Electrochim. Acta* 2014, **119**, 114.
6 Morozov, S. V; Novoselov, K. S.; Katsnelson, M. I.; Schedin, F.; Elias, D. C.; Jaszczak, J. A.; Geim, A. K. *Phys. Rev. Lett.* 2008, **100**, 16602.
7 Park, S.; Ruoff, R. S. *Nat. Nanotechnol.* 2009, **4**, 217.
8 Alwarappan, S.; Erdem, A.; Liu, C.; Li, C.-Z. *J. Phys. Chem. C* 2009, **113**, 8853.
9 Brownson, D. a. C.; Munro, L. J.; Kampouris, D. K.; Banks, C. E. *RSC Adv.* 2011, **1**, 978.
10 Goh, M. S.; Pumera, M. 2010, **82**, 8367.
11 Sheng, Z.-H.; Zheng, X.-Q.; Xu, J.-Y.; Bao, W.-J.; Wang, F.-B.; Xia, X.-H. *Biosens. Bioelectron.* 2012, **34**, 125.
12 Karlický, F.; Kumara Ramanatha Datta, K.; Otyepka, M.; Zbořil, R. *ACS Nano* 2013, **7**, 6434.
13 Georgakilas, V.; Otyepka, M.; Bourlinos, A. B.; Chandra, V.; Kim, N.; Kemp, K. C.; Hobza, P.; Zboril, R.; Kim, K. S. *Chem. Rev.* 2012, **112**, 6156.
14 Gong, P.; Wang, Z.; Li, Z.; Mi, Y.; Sun, J.; Niu, L.; Wang, H.; Wang, J.; Yang, S. *RSC Adv.* 2013, **3**, 6327.
15 Robinson, J. T.; Burgess, J. S.; Junkermeier, C. E.; Badescu, S. C.; Reinecke, T. L.; Perkins, F. K.; Zalalutdniov, M. K.; Baldwin, J. W.; Culbertson, J. C.; Sheehan, P. E.; Snow, E. S. *Nano Lett.* 2010, **10**, 3001.
16 Chantharasupawong, P.; Philip, R.; Narayanan, N. T.; Sudeep, P. M.; Mathkar, A.; Ajayan, P. M.; Thomas, J. *J. Phys. Chem. C* 2012, **116**, 25955.

17 Mathkar, A.; Narayanan, T. N.; Alemany, L. B.; Cox, P.; Nguyen, P.; Gao, G.; Chang, P.; Romero-Aburto, R.; Mani, S. a.; Ajayan, P. M. *Part. Part. Syst. Charact.* 2013, **30**, 266.

18 Sheets, M. G.; Li, W.; Tan, C.; Lowe, M. A. 2011, 2264.

19 Brownson, D. a C.; Gómez-Mingot, M.; Banks, C. E. *Phys. Chem. Chem. Phys.* 2011, **13**, 20284.

20 Lim, C. X.; Hoh, H. Y.; Ang, P. K.; Loh, K. P. *Anal. Chem.* 2010, **82**, 7387.

21 Gómez-Navarro, C.; Meyer, J. C.; Sundaram, R. S.; Chuvilin, A.; Kurasch, S.; Burghard, M.; Kern, K.; Kaiser, U. *Nano Lett.* 2010, **10**, 1144.

22 Shao, Y.; Wang, J.; Wu, H.; Liu, J.; Aksay, I. A.; Lin, Y. *Electroanalysis* 2010, **22**, 1027.

23 Brownson, D. a C.; Kampouris, D. K.; Banks, C. E. *Chem.Soc.Rev* 2012; **41**, 6944.

24 Ambrosi, A.; Chua, C. K.; Bonanni, A.; Pumera, M. *Chem. Mater.* 2012, **24**, 2292.

25 Ambrosi, A.; Bonanni, A.; Sofer, Z.; Cross, J. S.; Pumera, M. *Chemistry* 2011, **17**, 10763.

26 Ji, X.; Banks, C. E.; Crossley, A.; Compton, R. G. *Chemphyschem* 2006, **7**, 1337.

27 Pumera, M. *Chem. Rec.* 2009, **9**, 211.

28 Chia, X.; Ambrosi, A.; Otyepka, M.; Zbořil, R.; Pumera, M. *Chemistry* 2014, **20**, 1.

29 Acik, M.; Chabal, Y. J. *Jpn. J. Appl. Phys.* 2011, **50**, 070101.

30 Deakin, M. R.; Kovach, P. M.; Stutts, K. J.; Wightman, R. M. *Anal. Chem.* 1986, **58**, 1474.

31 Poh, H. L.; Šimek, P.; Sofer, Z.; Pumera, M. *Chemistry* 2013, **19**, 2655.

32 Tang, L.; Wang, Y.; Li, Y.; Feng, H.; Lu, J.; Li, J. *Adv. Funct. Mater.* 2009, **19**, 2782.

33 Romero-Aburto, R.; Narayanan, T. N.; Nagaoka, Y.; Hasumura, T.; Mitcham, T. M.; Fukuda, T.; Cox, P. J.; Bouchard, R. R.; Maekawa, T.; Kumar, D. S.; Torti, S. V; Mani, S. a; Ajayan, P. M. *Adv. Mater.* 2013, **25**, 5632.